Published in final edited form as:

J Environ Sci Health A Tox Hazard Subst Environ Eng. 2018 March 21; 53(4): 295–309. doi: 10.1080/10934529.2017.1400793.

Effects of Fuel Components and Combustion Particle Physicochemical Properties on Toxicological Responses of Lung Cells

Isabel C. Jaramillo[1], **Anne Sturrock**[2], **Hossein Ghiassi**[1], **Diana J. Woller**[2], **Cassandra E. Deering-Rice**[3], **JoAnn S. Lighty**[4], **Robert Paine**[2], **Christopher Reilly**[3], and **Kerry E. Kelly**[1,*]

[1]Department of Chemical Engineering, University of Utah, Salt Lake City, UT, United States of America

[2]Department of Pulmonary Medicine, University of Utah, Salt Lake City, UT, United States of America

[3]Department of Pharmacology and Toxicology, University of Utah, Salt Lake City, UT, United States of America

[4]Department of Mechanical and Biomedical Engineering, Boise State University, Boise, ID, United States of America

Abstract

The physicochemical properties of combustion particles that promote lung toxicity are not fully understood, hindered by the fact that combustion particles vary based on the fuel and combustion conditions. Real-world combustion-particle properties also continually change as new fuels are implemented, engines age, and engine technologies evolve. This work used laboratory-generated particles produced under controlled combustion conditions in an effort to understand the relationship between different particle properties and the activation of established toxicological outcomes in human lung cells (H441 and THP-1). Particles were generated from controlled combustion of two simple biofuel/diesel surrogates (methyl decanoate and dodecane/BD, and butanol and dodecane/AD) and compared to a widely studied reference diesel particle (NIST SRM2975/RD). BD, AD, and RD particles exhibited differences in size, surface area, extractable chemical mass, and the content of individual polycyclic aromatic hydrocarbons (PAHs). Some of these differences were directly associated with different effects on biological responses. BD particles had the greatest surface area, amount of extractable material and oxidizing potential. These particles and extracts induced cytochrome P450 1A1 and 1B1 enzyme mRNA in lung cells. AD particles and extracts had the greatest total PAH content and also caused CYP1A1 and 1B1 mRNA induction. The RD extract contained the highest relative concentration of 2-ring PAHs and stimulated the greatest level of interleukin-8 (IL-8) and tumor necrosis factor-alpha (TNFα) cytokine secretion. Finally, AD and RD were more potent activators of TRPA1 than BD, and while neither the TRPA1 antagonist HC-030031 nor the antioxidant N-acetylcysteine (NAC) affected

*Address correspondence to Kerry E. Kelly, Assistant Professor, University of Utah 2282 MEB, 50 S. Central Campus Dr., Salt Lake City, UT 84112; Phone: (801) 587-7601; Fax: (801) 585-9297; kerry, Kelly@utah.edu.

CYP1A1 or 1B1 mRNA induction, both inhibitors reduced IL-8 secretion and mRNA induction. These results highlight that differences in fuel and combustion conditions affect the physicochemical properties of particles, and these differences, in turn, affect commonly studied biological/toxicological responses.

Keywords

Combustion particle; soot; health effects; lung cells; TRPA channel; physicochemical properties; inflammatory response; oxidative potential

Introduction

Combustion-derived particle matter (cdPM) is a significant contributor to fine and ultrafine ambient PM (10–70% of $PM_{2.5}$).[1–3] Numerous studies have linked cdPM to adverse health effects including local and systemic inflammation, tissue damage, cancer, alterations to cardiopulmonary physiology, and development and exacerbation of chronic lung diseases.[1,4–7] However, the relationships between cdPM physicochemical properties and biological/toxicological responses remain incompletely understood. Recent efforts to reduce cdPM emissions and the overall carbon footprint of fossil fuels include the development of new engine technologies, PM filters, and biofuels.[8] The U.S. Energy Information Administration (EIA) projects that bio-derived fuels will increase annually by approximately 11% through 2040.[9] Two common classes of biofuels are alcohol-blended fuels (i.e., ethanol, butanol) and biodiesels, which consists of mono-alkyl esters of fatty acids (typically methyl esters); biodiesels can be used alone, without blending. Differences in fuel can have a significant effect on cdPM properties, including size distribution, surface area, ability to generate reactive oxygen species, and volatile content.[10–13]

Although the combustion of biofuels generally produces lower PM emissions than conventional petro-fuels, [14,15] some studies report that biofuels may modify emissions in ways that could adversely impact health as a result of increased particle-bound organic carbon content[16] and a higher respirable particle count,[16,17] due to a smaller mean particle diameter.[18,19] Furthermore, the higher oxygen content in biodiesel may lead to more reactive semi-volatile species and PM with greater oxidative potential.[20–22] For instance, some studies have reported that biodiesel PM is more reactive and affects lung cells to a greater degree than petroleum-based fuels.[22–26] Conversely, several studies suggest that biofuel-derived PM is comparable or less deleterious.[27–29]

Studying the potential health effects of cdPM derived from commercial engines using commercial fuels, regardless of origin, is often complicated by variations in combustion conditions, exhaust system conditioning, lubricants and variations in the composition of the commercial fuels. For example, differences in engine operating conditions, fuel, and exhaust system conditioning can all substantially modify the effects of cdPM on cardiac and inflammatory responses in animal models and human subjects.[30–34] These factors likely contribute to the contradictory results reported in the literature regarding the effects of diesel and biodiesel cdPM in biological systems. In fact, McDonald et al.[30] concluded that PM

mass concentration alone is an inadequate metric for comparing results among diesel exhaust studies conducted under different conditions of engine type and operation. Our study focused on one variable, differences in fuel, and it is intended to complement engine studies that compare bio-derived and petroleum-based fuels. It utilized particles and particle extracts generated from controlled combustion of two simple biofuel/diesel surrogates (methyl decanoate and dodecane, BD, and butanol and dodecane, AD), to address toxicological effects related to environmental cdPM variability. These cdPM and extracts were also compared to a widely studied reference petro-diesel particle (NIST SRM2975; RD). Additionally, this study focused on the role of specific cdPM physicochemical properties, on the activation of a set of toxicologically relevant endpoints using human H441 and THP1 cells as models. The following biological outcomes were evaluated: cytochrome P450 (CYP) 1A1 and 1B1 mRNA induction, enzymes that both detoxify and bioactivate polycyclic aromatic hydrocarbons (PAHs) in human airway epithelial cells[35–37]; secretion of interleukin-8 (IL-8) and tumor necrosis factor-alpha (TNFα, proteins that regulate host-defenses and inflammation) [35,38,39]; activation of transient receptor potential ankyrin-1 (TRPA1), a protein that triggers irritation sensations and the cough reflex via C-fibers, as well as inflammation and edema[40,41]; and oxidizing potential (oxidative stress induced by cdPM is believed to be a cause of many adverse biological effects). Finally, the role of specific cdPM physicochemical properties and their effects on different biological processes were evaluated using a combination of standardized PAH samples and inhibitors of both TRPA1 and oxidative stress.

Materials and methods

cdPM Generation and Collection

PM from two different liquid fuel mixtures, BD and AD, were generated in a fuel-rich, premixed, flat-flame burner (FFB) which operates at atmospheric pressure (Fig. S1). This setup allows for the generation of reproducible particles from defined fuels.[42–49] It allows for the exploration of how cdPM physicochemical properties affect toxicological responses by eliminating some of the confounding effects associated with inconsistencies in engine conditions and fuels, and it can complement studies of engine exhaust. To produce cdPM for this study, the liquid–fuel mixture was injected into a vaporizer (V-1, Fig. S1) using a syringe pump (KDS-410). Vaporized fuel mixed with air and flowed into the bottom of the burner. A 25-mm thick bed of mixing beads inside the burner chamber completed the mixing. The temperature in the vaporizer and along the feeding line was maintained above 120°C to avoid condensation. The composition of the fuel mixture was confirmed by gas chromatography before and after vaporization to verify that the fuel was not distilled upon vaporization. The flame was stabilized over a tube bundle through which the mixture passed in laminar flow. The particle sampling system consisted of a paper filter media (pore size 0.2 μm) fitted into a filter holder installed in the sampling line. The temperature inside the filter holder was maintained between 120-160°C to avoid water condensation. A pump provided constant suction through the sampling line. Particles deposited on the paper filter were recovered by scraping and subsequently used in the biological assays.

Consistent combustion conditions were maintained with a carbon oxygen ratio (C/O ratio) of 1.13. The C/O ratio of the oxygenated fuels included not only the oxygen in the oxidizer but also the oxygen present in the fuel. The fuel mixtures consisted of: (1) 30% mol *n*-butanol and 70% mol *n*-dodecane (AD, representing an alcohol blended diesel) and (2) 30% mol methyl decanoate and 70% mol *n*-dodecane (BD, representing a biofuel-blended diesel). Flame temperatures were measured for both fuel blends using a type-B thermocouple (wire diameter = 0.002032 cm) and corrected for radiation [50]. The particle samples were collected at the height above the burner at which the temperature profiles for both fuel blends were similar and have roughly a temperature of 1400°C.

In addition to the cdPM generated in the flat flame, a widely studied commercial reference diesel PM, originally collected from an industrial diesel-powered forklift (NIST 2975, RD), was also studied.

Particle Characterization

Particle size distributions (PSDs) were measured for the flame particle samples utilizing a scanning mobility particle sizer (SMPS) (Supplemental Fig. S2). The SMPS classifies charged particles according to their mobility in an electric field. The total integrated surface area was directly calculated from the size and number concentrations of the measured PSDs assuming spherical particles. The product of mobility diameter and the equivalent particle number density was integrated over the range of mobility diameters to obtain the surface area representative of the measured PSD. This method is commonly used to estimate the surface area of combustion particles, and it agrees well with the Brunauer, Emmett, Teller measurements of surface area at low mobility sizes (below 200 nm in diameter).[51–54] The median particle size for RD was estimated by transmission electron microscopy (TEM) images, and the surface area was provided from the NIST certificate of analysis.[55]

PM generated from the different fuels and combustion conditions was extracted to release particle-associated chemicals. These extracts were used to treat cells and were evaluated for differences in the amount of extractable organic material. Ethanol-soluble compounds associated with the particles were extracted from 25 mg of cdPM sample by suspending the cdPM in 15 mL of ethanol and sonicating in a water bath for 2h. The samples were then centrifuged at 10,000 x*g* for 5 min and the supernatant filtered through a 0.22 μm syringe filter 2× to remove the insoluble PM. The extracts were dried under nitrogen and stored at -80°C until use.

The cdPM extracts were sent to an external laboratory for chemical analysis of PAHs using gas chromatography/mass spectrometry (GC/MS) in accordance with EPA method 8270. The identification of the target compounds was based on the detection of the molecular ion along with comparison of analyte retention time relative to that of the PAH standards. An EPA 16 priority PAH mixture was used as an analysis standard and as a standard extract in selected biological tests. This mixture contained 16 PAHs, each at a concentration of 2000 μg/mL, in a methylene chloride solution (EPA 610- Restek, Bellefonte, PA). For biological experiments, the methylene chloride was first evaporated and the PAH residue reconstituted in DMSO to the desired stock concentration.

Lung Cell Lines

NCI-H441 and THP-1 cells were obtained from ATCC (Manassas, VA) and maintained in RPMI +10% fetal calf serum. H441 cells are a human small airway carcinoma cell line with non-ciliated airway epithelial/Club cell characteristics. H441 cells were used to model cdPM interactions with the distal airway/bronchiolar epithelial cells. [56,57] THP-1 cells are a pro-monocytic cell line that is differentiated to pulmonary macrophage-like cells, as described by Daigneault et al. [58,59]

Cell Treatments

Cells were exposed to cdPM and/or cdPM extracts at 80% confluence in fresh growth media. cdPM was suspended and sonicated in culture media immediately before addition to the cells at an area doses of up to 50 μg/cm^2 (200 μg/mL). cdPM extracts were solubilized in DMSO at a concentration of 6 mg/mL and diluted so that cells were treated with an identical area dose of residue and DMSO. However, an equal mass for the residues represented different amounts of original PM because each PM type has a different fraction of soluble material (Table 1). Immediately prior to addition to the cells, the stock solution was diluted in cell culture media to achieve an area dose of 12.5 μg/cm^2 (50 μg/mL). An exposure time of 24h was used to capture short-term, acute responses induced by the various particle samples. The negative control for all experiments was cells treated with media containing DMSO (0.1% v/v).

Cells were also exposed to the PAH mixture to evaluate the contributions of PAHs to selected biological outcomes, including secretion of IL-8 and TNFα protein, CYP 1A1 and 1B1 mRNA expression, and TRPA1 activation. The solution was dried and re-constituted in DMSO. Cells were then exposed to the mixture to yield area doses of 12.5 and 25 μg/cm^2 (50 and 100 μg/mL).

Cytotoxicity Assays

cdPM-induced cytotoxicity was determined by measuring the cells metabolic/mitochondrial activity (mitochondrial reductase activity) following 24h treatment using the MTT assay (Promega, Madison, WI) according to the manufacturer's protocol. Lactate dehydrogenase release and trypan blue exclusion assays were also used to verify the MTT assay results.

Real-Time Quantitative (qPCR) Analysis of CYP1A1 and 1B1 mRNA Expression

CYP1A1 and CYP1B1 mRNA transcript levels were measured in H441 and THP-1 cells using qPCR in response to both cdPM and cdPM extract treatments. TRPA1 mRNA was also assayed in untreated cells. Total RNA was isolated using the RNeasy kit (Qiagen). cDNA was prepared using the High Capacity cDNA Reverse Transcription kit (Applied Biosystems), and amplification of target genes was performed using a PikoReal Thermocycler (ThermoFisher) using a 2-step program (Tm= 60°C) with dissociation analysis. Gene specific primers were designed using the Roche Applied Science Universal Probe Library Assay Design Center and were as follows: Human CYP1A1 Forward 5′-TCCAAGAGTCCACCCTTCC-3′ and Reverse 5′-AAGCATGATCAGTGTAGGGATCT-3′; Human CYP1B1 Forward 5′-

ACGTACCGGCCACTATCACT-3′ and Reverse 5′-CTCGAGTCTGCACATCAGGA-3′; Human TRPA1 Forward 5′-TCACCATGAGCTAGCAGACTATTT-3′ and Reverse 5′-GAGAGCGTCCTTCAGAATCG-3′; and Human GAPDH Forward 5′-AGCCACATCGCTCAGACAC-3′ and Reverse 5′-GCCCAATACGACCAAATCC-3′. A no template control was included in each experiment. Each biological sample (n=3) had two technical replicates that were averaged for statistical analysis. Data were analyzed using ΔΔCt and normalized to GAPDH. Data are represented as fold change versus the untreated control group.

IL-8 and TNFα ELISA

Secretion of IL-8 and TNFα protein by cells in response to cdPM, cdPM extract and PAH mixture treatment was measured by ELISA (R&D Systems), according to the manufacturer protocols. These two measures of inflammation were selected for the two different cells because H-441 cells do not secrete significant quantities of TNFα proteins and THP cells have high background of IL-8 proteins. All media samples were cleared of cellular debris and any insoluble agonist or particles, aliquoted and frozen. The measurements were carried out on media samples that had under gone one freeze thaw cycle.

TRPA1 Activation

Activation of TRPA1 by cdPM and cdPM extracts was evaluated by quantifying changes in intracellular calcium content in human TRPA1-overexpressing HEK-293 cells using the Fluo-4 Direct assay kit (Invitrogen, Carlsbad, CA), as previously described [40,41]. Data are represented as the percentage of the maximum change in cellular fluorescence achieved by ionomycin treatment (10 μM) and normalized to responses elicited by a positive control (allyl-isothiocyanate, 150 μM). To determine TRPA1 involvement in the biological effects of cdPM, lung cells were co-treated with the TRPA1 antagonist HC-030031 (25 μM).

Oxidative Potential

The oxidative potential of the cdPM extracts was measured using an *in vitro* dithiothreitol (DTT) oxidation assay.[60] cdPM extracts consume a fixed quantity of DTT over a defined incubation period and the remaining reduced DTT was then quantified spectrophotometrically by absorbance at 415 nm following reaction with 5,5′ -dithiobis-2-nitrobenzoic acid (DTNB) to yield the product 2-nitro-5- mercaptobenzoic acid. To determine the involvement of cdPM associated oxidants/electrophiles in cellular responses to the cdPM and cdPM extracts, the glutathione precursor and antioxidant N-acetylcysteine (NAC) was used. NAC (10mM) was made fresh in culture media (RPMI) immediately prior to addition to the cells and adjusting the pH to 7.2 with NaOH. The media was then filtered using a 0.22 micron filter.

Data Analysis

Statistical analysis was performed by one-way or two-way analysis of variance (ANOVA) using Graphpad 5 software. One-way ANOVA with Tukey's honestly significant difference (HSD) post hoc test was performed to compare differences between all sample means except for TRPA1 activation by particle extracts. This evaluation included two concentrations and

three particle-extract types, and two -way ANOVA was performed with Dunnett's a post-hoc analysis. Comparisons were made between control and treated groups as noted in figure legends.

Results

cdPM Size, Surface Area and Composition

cdPM produced by the two different fuels, BD and AD, in the FFB resulted in PM with different sizes and surface areas (Table 1). The median particle size for AD (41 ± 5 nm) was greater than that for BD and RD (26 ± 3 nm and 28 ± 3 nm, respectively). These mean particle sizes are in the range of those commonly reported in engine studies. [61–63] The relative surface area was greatest for BD (384 m^2/g), followed by AD (125 m^2/g) and RD (80 m^2/g).

cdPM is composed of carbon soot with variable levels of adsorbed organic materials. Here, the percentage of extractable material content was greatest for BD (~20% w/w) followed by AD (~12%) and RD (~8%) (Table 1). Thus, a 12.5 μg/cm^2 area dose of particles (used in the biological effect assays) was equivalent to a 2.5, 1.5, or 1 μg/cm^2 area dose of extract for BD, AD, and RD, respectively. Similarly, a cdPM extract area dose of 12.5 μg/cm^2 cdPM would represent area doses of 62.5, 104, and 156 μg/cm^2 BD, AD, and RD, respectively.

The relative concentrations of PAHs also vary among the three cdPM evaluated in this study (Table 2). These PAHs have been commonly evaluated in previous studies of diesel engine exhaust.[64,65] The overall PAH content was greatest for AD (92.61 μg/g) and comparable for BD and RD (66.43 and 62.95 μg/g). Of note, BD and AD contained a greater percentage 5-ring PAHs (benzo[a]pyrene in particular) than RD. AD contained the highest percentage (~40%) of 4-ring PAHs (i.e., fluoranthene and pyrene), and RD contained the highest percentage (~9%) of 2-ring PAHs (naphthalene). Table S1 provides correlations between cdPM size, surface area and composition.

cdPM Cytotoxicity

PM are often reported to be cytotoxic to lung cells. However, neither the cdPM nor the cdPM extracts caused cytotoxicity with 24h treatment at area doses up to 50 μg/cm^2 (200 μg/mL), as measured in the MTT assay (Fig. S3), by lactate dehydrogenase release or in trypan blue exclusion assays (data not shown).

Expression of CYP1A1 and 1B1 mRNA in H441 and THP-1 Cells

The ability of cdPM to induce CYP1A1 and 1B1 gene expression is widely reported in the literature. In this study, up to ~100-fold up-regulation of CYP1A1 mRNA and up to ~30-fold up-regulation of CYP1B1 mRNA was observed in H441 cells treated with an equal area dose of either cdPM or cdPM extracts (Fig. 1A-D). In general, the cdPM and their respective extracts promoted similar relative levels of expression. The relative level of mRNA up-regulation was greatest for BD cdPM and the BD extract, followed by RD and AD. Interestingly, for AD, up-regulation was only observed using the AD extract. CYP1A1 and

1B1 mRNA up-regulation was also observed in THP-1 cells, albeit at lower levels compared to H441 cells, with essentially the same profile as that for H441 cells (Fig. S4A-D).

IL-8 and TNFα Cytokine Secretion

Secretion of pro-inflammatory cytokines in lung cells by cdPM is also widely reported in the literature. All three cdPM and their extracts stimulated IL-8 cytokine secretion by H441 cells (Figs 2A and B) and TNFα cytokine secretion by THP-1 cells (Figs 2C and D). In H441 cells, RD was the most effective and AD the least effective stimulus of IL-8 cytokine secretion. The THP-1 cells showed a similar trend for TNFα release, where RD was most and AD was the least effective. Note, the three different cdPM exhibited a different rank order for the secretion of IL-8 and TNFα cytokines than for CYP1A1 and 1B1, presumably indicating a different biochemical mechanism underlying these cellular responses.

TRPA1 Activation by cdPM

The human TRPA1 ion channel has previously been identified as a target of cdPM.[40] TRPA1 was also differentially activated by the cdPM (Fig. 3A) and cdPM extracts (Fig. 3B). RD particles activated TRPA1, but neither BD nor AD particles activated TRPA1 using an area dose of 180 μg/cm^2 (equivalent to a suspension of 2.3 mg/mL in a single well of a 96-well plate) and an assay duration of 1 min (Fig. 3A,B). However, all three cdPM extracts activated TRPA1, at area doses of 90 (1.15 mg/mL) and 180 μg/cm^2 (2.3 mg/mL), with RD and AD extracts showing similar potency and greater than that of BD (Fig. 3B).

Role of TRPA1 and PAHs in IL-8 Secretion and CYP1A1/1B1 mRNA Expression in H441 Cells

All three cdPM extracts contained substantial quantities of PAHs (Table 2), induced CYP1A1 and 1B1 mRNA, and stimulated IL-8 cytokine secretion by H441 cells. The immunomodulatory effects of aryl-hydrocarbon receptor (AhR) agonists (PAHs) and oxidants are known, but possible roles of TRPA1 have not been widely studied. TRPA1-mediated calcium influx in lung cells was therefore tested as a basis for CYP1A1 and 1B1 mRNA expression, and IL-8 cytokine secretion. Expression of TRPA1 mRNA was confirmed in H441 cells by qPCR (data not shown). Stimulation of IL-8 cytokine secretion by cdPM extracts was attenuated by the TRPA1 antagonist HC-030031, with the proportion of inhibition for the AD, BD, and RD extracts (~20%, 10%, 30%, respectively), roughly paralleling the relative potency of these extracts as TRPA1 agonists (Fig. 4A). Similar to the cdPM, an EPA 16 PAH mixture also stimulated IL-8 cytokine secretion by H441 cells, and IL-8 cytokine secretion by the PAH mixture was also attenuated ~60% by HC-030031 (Fig. 4B), despite the PAH mixture not showing activation of TRPA1 in short-term calcium flux assays (data not shown). This suggests that factors beyond PAH content are involved in TRPA1 mRNA expression. A role for TRPA1 in CYP1A1 and 1B1 mRNA expression by the cdPM, cdPM extracts, and the PAH mixture was also evaluated (Fig. 5A-C); co-treatment of cells with HC-030031 had no effect on CYP1A1 or 1B1 mRNA expression by AD, BD or RD cdPM (Fig. 5A), the respective cdPM extracts (Fig. 5B), or the mixture of PAHs (Fig. 5C), also suggesting different pathways leading to the up-regulation of these genes.

Oxidative Potential of cdPM and Roles in H441 Responses

cdPM and other environmental particles are widely believed to affect biological processes through oxidative and/or electrophile stress. [66–69] All three cdPM extracts oxidized DTT, but to a different extent (Fig. 6A). AD and BD oxidized ~6% and 15% DTT, respectively, in 30 minutes, while in the same time period RD oxidized only ~4%. The role of oxidative/electrophile stress in cellular responses to the cdPM was also further explored (Fig. 6B-D). Pre-treatment of H441 cells with the glutathione precursor and ROS/electrophile scavenger, NAC, was used. NAC partially, but significantly, reduced CYP1A1 and 1B1 mRNA expression by H441 cells in response to both BD and AD, and completely inhibited the response to RD (Fig. 6B and 5C). Furthermore, stimulation of IL-8 cytokine secretion by all three cdPM extracts was suppressed by NAC (Fig. 6D).

Discussion

The size, shape, soluble organic fraction and chemical composition, and oxidative potential and electrophile content, are all widely reported to influence the biological effects of cdPM and other environmental particles.[39] Combusting two different precisely defined fuels (BD and AD) under identical conditions resulted in particles and extracts with significant differences in their physicochemical properties, including differences in size, surface area, extractable chemical content, total and relative PAH content, and oxidizing potential/electrophile content. These differences manifested as variable effects on lung cells using a panel of relevant toxicological endpoint assays. The two FFB-generated particles and extracts also exhibited differences when compared to RD particles in terms of their extractable content, PAH composition, and effects on toxicological endpoints and lung cells.

From a toxicological/human health effects standpoint, the results of this study confirm that cdPM components, principally PAHs associated with the cdPM, are inducers of CYP1A1 and 1B1 mRNA expression. Further, the ability to affect CYP expression varies as a function of particle properties (Fig. 1 and S4). Lung cells treated with cdPM, such as diesel PM, often show increased expression of CYP1A1 and 1B1.[70,71] The up-regulation of CYP1A1 and 1B1 mRNA in response to cdPM may have important consequences such as protection of cells through enhanced metabolic clearance of toxins, or deleterious effects via bioactivation of inhaled pro-toxicants to toxic metabolites capable of damaging biological macromolecules and causing cellular injury (e.g., benzo[a]pyrene and DNA damage, or napthlalene toxicity).[67,72,73]

Differences in PAH profiles for different fuel-derived particles have been reported by others. [27,74,75] For example, Sadiktsis [74] investigated particle-associated PAHs from three different fuels: biodiesel B100, B30 bio-diesel blend, and petro-diesel. They found that B30 had a lower total PAH content than petroleum diesel fuel, but particles from biodiesel contained a higher percentage of selected higher molecular weight PAHs. In this study PAHs were abundant in all three cdPM extracts, but AD particles had the greatest total PAH content, ~30% more per gram than either BD or RD. However, CYP1A1 and 1B1 mRNA up-regulation did not correlate with total PAH content (R^2=<0.2). Rather, from Table 2 it appeared that the relative content of selected 4- and 5-ring PAHs, which are known to be

more potent AhR agonists[76] ultimately correlated with the relative potency of the cdPM materials and extracts. CYP1A1 and 1B1 also correlated with extractable organic content, with R^2 values of 0.888 and 0.887. As such, we propose that the relative strength of BD in stimulating CYP1A1/1B1 transcription was associated with the relatively high surface area, extractable chemical content, and the abundance of selected PAHs that activate the AhR. To this end, a soluble mixture of 16 PAHs also caused significant induction of CYP1A1 and 1B1 mRNA (Fig. 5C).

Pro-inflammatory cytokine production by lung cells is another common response to cdPM exposure.[39] Prior studies have reported that organic extracts of traffic-related PM [77], such as RD and other diesel exhaust PM [23,78–81], were involved in IL-8 and TNFα cytokine secretion by human lung cells. The three cdPM particles and extracts used in this study exhibited variable activity, with RD particles and extracts stimulating the greatest cytokine secretion of IL-8 and TNFα from both H441 and THP-1 cells. The RD extract had the lowest level of extractable chemical content of all three cdPM (~8% w/w), yet it was the most potent for IL-8 and TNFα cytokine secretion by the lung cells, essentially opposite from the CYP induction response. From Table 2, RD contained the highest relative concentration of 2-ring PAHs (i.e., naphthalene), suggesting that this specific property may be a key mediator of IL-8 and TNFα cytokine secretion in these cells (R^2=0.563).

Activation of TRP channels in lung cells has previously been shown to influence lung cell responses to cdPM.[40,41,82] TRPA1 is a calcium ion channel that is activated by a variety of cdPM, including diesel exhaust PM and extracts.[40] Disruption of intracellular calcium homeostasis is a mechanism for cytokine gene induction, often through the NF-kB signaling pathway. Therefore, TRPA1 was tested as mechanism contributing to the cdPM effects on lung cells. RD particles activated TRPA1, as previously reported [40], but neither BD nor AD particles activated TRPA1 in the short-term calcium assays (Fig. 3A). As previously reported, TRPA1 activation by diesel exhaust PM was increased by prior extraction of specific reactive chemicals from diesel exhaust PM.[40] Accordingly, all three extracts were TRPA1 agonists (Fig. 3B), with RD and AD exhibiting greater potency than BD. This pattern was inversely related to the total extractable content of the cdPM, suggesting that specific chemical components of the extracts, rather than total extractable organic content, was responsible for TRPA1 activation versus the total amount of extractable material.

IL-8 cytokine secretion by lung epithelial cells, such as H441 cells, is a common effect of cdPM treatment. However, biochemical mechanisms underlying this response have not been fully delineated. Here the results show that stimulation of IL-8 cytokine secretion by the cdPM was attenuated by the TRPA1 antagonist HC-030031 (Figs 4 and BA), with the relative proportion of inhibition roughly paralleling the relative potency of these materials as TRPA1 agonists. To further understand the relationship between TRPA1 and stimulation of IL-8 secretion, the chemical compositions of the cdPM extracts were also considered. RD contained the highest abundance of 2- and 3-ring PAHs (23.3 μg/g), compared to AD and BD (16.8 μg/g and 13.6 μg/g, respectively) (Table 2). RD consistently produced the largest increases in IL-8 cytokine secretion, and this response was largely inhibited by the TRPA1 antagonist. As such, these data suggest that TRPA1 may contribute to IL-8 cytokine

secretion by the cdPM and PAH mixture. Further, TRPA1 activation also correlated well with CYP up-regulation (R^2=0.98 and 0.996 for 1A1 and 1B1, respectively) suggesting that CYP-mediated metabolism of lower molecular weight PAHs to electrophiles (e.g., quinones) over the 24-hour experimental period may be important in the apparent IL-8/TRPA1 association. While not directly tested here, this hypothesis is consistent with the report by Lanosa et al. [83] who showed that TRPA1 activation in mouse airways/lungs by naphthalene was dependent upon CYP-mediated bioactivation. Further, we have shown previously that 1,2-napthoquinone (and similar oxy-PAHs), but not naphthalene itself was a potent TRPA1 agonist.[40] Finally, consistent with different mechanisms for IL-8 cytokine secretion versus CYP mRNA expression, TRPA1 did not play a role in CYP1A1 or 1B1 mRNA up-regulation (Figs 5A and B) indicating selective effects of TRPA1 activation in lung cells, independent of AhR.

Prior studies have also demonstrated the ability of a variety of cdPM to promote oxidative stress *in vitro*, and correlations between oxidative potential and various biological effects including cytotoxicity and cytokine production have been reported.[66,69,84] The oxidative potential of BD was more than double of that of AD and RD (Fig. 6A), but in this study, there were no observable differences in the cytotoxicity of the cdPM or extracts. However, oxidative potential did correlate with CYP up-regulation (R^2=0.979 and 0.974 for 1A1 and 1B1, respectively), but to a lesser extent (R^2=0.2 and 0.26) for IL-8 and TNFα cytokine secretion. However, the antioxidant and glutathione precursor NAC did abrogate IL-8 production (Fig. 6D), and partially suppressed CYP1A1 and 1B1 up-regulation elicited by AD and BD (Figs 6B and C). These results suggest that the effects of these cdPM on lung cells were likely, in part, dependent on oxidative stress and/or electrophiles, which in the case of IL-8 cytokine secretion likely involve activation of TRPA1 by oxidants and electrophiles both present on the cdPM as well as those generated by CYP-mediated metabolism.

Conclusion

This study investigated the role of cdPM physicochemical properties on several toxicologically relevant outcomes in lung cells. The approach, which used well-defined particles and toxicological endpoint assays, was advantageous in that it facilitated the identification of potentially important biochemical mechanisms by which cdPM, such as diesel exhaust PM, may affect lung cells. The results of this study highlight that differences in fuel composition, which results in differences in particle characteristics, can lead to meaningful differences in the physicochemical properties of particles. In turn, these differences can have marked effects on the activation of commonly studied toxicological responses. The results suggest that these differences in cdPM properties, in particular surface area and extractable chemical composition, adds to the complexity of response to particulate matter. As such, variations in cdPM properties should be carefully considered when testing mechanisms by which they affect different biological endpoints.

Supplementary Material

Refer to Web version on PubMed Central for supplementary material.

Acknowledgments

This material is based upon work supported by the National Science Foundation while J. S. Lighty served at the NSF. Any opinion, findings, and conclusions or recommendations expressed in this material are those of the author(s) and do not necessarily reflect the views of the National Science. This work was supported by a Merit Research Grant from the Department of Veterans Affairs [660-D64122] (R. Paine), the NIEHS [R01 ES017431] (C. Reilly), the NIEHS [5K25ES027504-02] and the NSF under Award Number 10023049 (K. Kelly and J. Lighty).

References

1. Jacobson MZ. Strong radiative heating due to the mixing state of black carbon in atmospheric aerosols. Nature. 2001; 409(6821):695–697. [PubMed: 11217854]
2. Zhang R, Khalizov AF, Pagels J, Zhang D, Xue H, McMurry PH. Variability in morphology, hygroscopicity, and optical properties of soot aerosols during atmospheric processing. Proc Natl Acad Sci USA. 2008; 105
3. Dellinger, B., D'Alessio, A., D'Anna, A., Ciajolo, A., Gullett, B., Henry, H., Keener, M., Lighty, J., Lomnicki, S., Lucas, D., et al. Report: Combustion Byproducts and Their Health Effects: Summary of the 10th International Congress. Vol. 25. Mary Ann Liebert, Inc; 140 Huguenot Street, 3rd FloorNew Rochelle, NY 10801USA: 2008.
4. Lighty JS, Veranth JM, Sarofim AF. Association Combustion Aerosols: Factors Governing Their Size and Composition and Implications to Human Health. J Air Waste Manage Assoc. 2000; 509(10):1565–1618. DOI: 10.1080/10473289.2000.10464197
5. Nemmar A, Dhanasekaran S, Yasin J, Ba-Omar H, Fahim MA, Kazzam EE, Ali BH. Evaluation of the direct systemic and cardiopulmonary effects of diesel particles in spontaneously hypertensive rats. Toxicology. 2009; 262:50–56. DOI: 10.1016/j.tox.2009.05.009 [PubMed: 19463885]
6. Ristovski ZD, Miljevic B, Surawski NC, Morawska L, Fong KM, Goh F, Yang IA. Respiratory health effects of diesel particulate matter. Respirology. 2012; 17(2):201–212. [PubMed: 22126432]
7. Benbrahim-Tallaa L, Baan RA, Grosse Y, Lauby-Secretan B, El Ghissassi F, Bouvard V, Guha N, Loomis D, Straif K. Carcinogenicity of diesel-engine and gasoline-engine exhausts and some nitroarenes. Lancet Oncol. 2016; 13(7):663–664. DOI: 10.1016/S1470-2045(12)70280-2
8. Gill SS, Turner D, Tsolakis A, York APE. Controlling soot formation with filtered EGR for diesel and biodiesel fuelled engines. Environ Sci Technol. 2012; 46(7):4215–4222. DOI: 10.1021/es203941n [PubMed: 22380527]
9. Annual Energy Outlook 2014 Early release Overview, D.-0383ER(2014). EIA (Energy Information Association);
10. Salvi AA, Assanis D, Filipi Z. Impact of physical and chemical properties of alternative fuels on combustion, gaseous emissions, and particulate matter during steady and transient engine operation. Energy and Fuels. 2012; 26(7):4231–4241. DOI: 10.1021/ef300531r
11. Lu T, Cheung CS, Huang Z. Investigation on Particulate Oxidation from a DI Diesel Engine Fueled with Three Fuels. Aerosol Sci Technol. 2012; 46(12):1349–1358. DOI: 10.1080/02786826.2012.713534
12. Kennedy IM. The health effects of combustion-generated aerosols. Proc Combust Inst. 2007; 31(2): 2757–2770. DOI: 10.1016/j.proci.2006.08.116
13. Martin N, Lombard M, Jensen KR, Kelley P, Pratt T, Traviss N. Effect of biodiesel fuel on “real-world”, nonroad heavy duty diesel engine particulate matter emissions, composition and cytotoxicity. Sci Total Environ. 2017; 586:409–418. DOI: 10.1016/j.scitotenv.2016.12.041 [PubMed: 28236480]
14. Xue J, Grift TE, Hansen AC. Effect of biodiesel on engine performances and emissions. Renew Sustain Energy Rev. 2011; 15(2):1098–1116. DOI: 10.1016/j.rser.2010.11.016

15. Lackey LG, Paulson SE. Influence of feedstock: Air pollution and climate-related emissions from a diesel generator operating on soybean, canola, and yellow grease biodiesel. Energy and Fuels. 2012; 26(1):686–700. DOI: 10.1021/ef2011904
16. Surawski NC, Miljevic B, Ayoko GA, Elbagir S, Stevanovic S, Fairfull-Smith KE, Bottle SE, Ristovski ZD. Physicochemical characterization of particulate emissions from a compression ignition engine: The influence of biodiesel feedstock. Environ Sci Technol. 2011; 45:10337–10343. DOI: 10.1021/es2018797 [PubMed: 22039912]
17. Shi X, He K, Zhang J, Ma Y, Ge Y, Tan J. A comparative study of particle size distribution from two oxygenated fuels and diesel fuel. Front Env Sci Eng China. 2010; 4(1):30–34.
18. Rahman MM, Pourkhesalian AM, Jahirul MI, Stevanovic S, Pham PX, Wang H, Masri AR, Brown RJ, Ristovski ZD. Particle emissions from biodiesels with different physical properties and chemical composition. FUEL. 2014; 134:201–208. DOI: 10.1016/j.fuel.2014.05.053
19. Tzamkiozis T, Ntziachristos L, Mamakos A, Fontaras G, Samaras Z. Aerodynamic and Mobility Size Distribution Measurements to Reveal Biodiesel Effects on Diesel Exhaust Aerosol. Aerosol Sci Technol. 2011; 45:587–595. DOI: 10.1080/02786826.2010.550961
20. Stevanovic S, Miljevic B, Surawski NC, Fairfull-Smith KE, Bottle SE, Brown R, Ristovski ZD. Influence of oxygenated organic aerosols (OOAs) on the oxidative potential of diesel and biodiesel particulate matter. Environ Sci Technol. 2013; 47:7655–7662. DOI: 10.1021/es4007433 [PubMed: 23763365]
21. Pourkhesalian AM, Stevanovic S, Salimi F, Rahman MM, Wang H, Pham PX, Bottle SE, Masri AR, Brown RJ, Ristovski ZD. Influence of fuel molecular structure on the volatility and oxidative potential of biodiesel particulate matter. Environ Sci Technol. 2014; 48:12577–12585. DOI: 10.1021/es503160m [PubMed: 25322332]
22. Fukagawa NK, Li M, Poynter ME, Palmer BC, Parker E, Kasumba J, Holmén Ba. Soy biodiesel and petrodiesel emissions differ in size, chemical composition and stimulation of inflammatory responses in cells and animals. Environ Sci Technol. 2013; 47:12496–12504. DOI: 10.1021/es403146c [PubMed: 24053625]
23. Swanson KJ, Kado NY, Funk WE, Pleil JD, Madden MC, Ghio AJ. Release of the Pro-Inflammatory Markers by BEAS-2B Cells Following In Vitro Exposure to Biodiesel Extracts. Open Toxicol J. 2009; 3(1):8–15. DOI: 10.2174/1874340400903010008
24. Bhavaraju L, Shannahan J, William A, McCormick R, McGee J, Kodavanti U, Madden M. Diesel and biodiesel exhaust particle effects on rat alveolar macrophages with in vitro exposure. Chemosphere. 2014; 104:126–133. DOI: 10.1016/j.chemosphere.2013.10.080 [PubMed: 24268344]
25. Shvedova AA, Yanamala N, Murray AR, Kisin ER, Khaliullin T, Hatfield MK, Tkach AV, Krantz QT, Nash D, King C, et al. Oxidative stress, inflammatory biomarkers, and toxicity in mouse lung and liver after inhalation exposure to 100% biodiesel or petroleum diesel emissions. J Toxicol Environ Health A. 2013; 76(15):907–921. DOI: 10.1080/15287394.2013.825217 [PubMed: 24156694]
26. Yanamala N, Hatfield MK, Farcas MT, Schwegler-Berry D, Hummer JA, Shurin MR, Birch ME, Gutkin DW, Kisin E, Kagan VE, et al. Biodiesel versus diesel exposure: Enhanced pulmonary inflammation, oxidative stress, and differential morphological changes in the mouse lung. Toxicol Appl Pharmacol. 2013; doi: 10.1016/j.taap.2013.07.006
27. Brito JM, Belotti L, Toledo AC, Antonangelo L, Silva FS, Alvim DS, Andre PA, Saldiva PHN, Rivero DHRF. Acute cardiovascular and inflammatory toxicity induced by inhalation of diesel and biodiesel exhaust particles. Toxicol Sci. 2010; 116(1):67–78. DOI: 10.1093/toxsci/kfq107 [PubMed: 20385657]
28. Krahl J, Bunger J, Schroder O, Munack A, Knothe G. Exhaust emissions and health effects of particulate matter from agricultural tractors operating on rapeseed oil methyl ester. Am Oil Chem Soc. 2002; 79(7):717–724.
29. Topinka J, Milcova A, Schmuczerova J, Mazac M, Pechout M, Vojtisek-Lom M. Genotoxic potential of organic extracts from particle emissions of diesel and rapeseed oil powered engines. Toxicol Lett. 2012; 212(1):11–17. DOI: 10.1016/j.toxlet.2012.04.017 [PubMed: 22562013]

30. McDonald JD, Campen MJ, Harrod KS, Seagrave J, Seilkop SK, Mauderly JL. Engine-operating load influences diesel exhaust composition and cardiopulmonary and immune responses. Environ Health Perspect. 2011; doi: 10.1289/ehp.1003101

31. Lucking AJ, Lundbäck M, Barath SL, Mills NL, Sidhu MK, Langrish JP, Boon NA, Pourazar J, Badimon JJ, Gerlofs-Nijland ME, et al. Particle Traps Prevent Adverse Vascular and Prothrombotic Effects of Diesel Engine Exhaust Inhalation in MenClinical Perspective. Circulation. 2011; 123(16):1721–1728. [PubMed: 21482966]

32. Farraj AK, Haykal-Coates N, Winsett DW, Gilmour MI, King C, Krantz QT, Richards J, Hazari MS. Comparative electrocardiographic, autonomic and systemic inflammatory responses to soy biodiesel and petroleum diesel emissions in rats. Inhal Toxicol. 2015; 27(11):564–575. DOI: 10.3109/08958378.2015.1057884 [PubMed: 26514784]

33. Saathoff H, Moehler O, Schurath U, Kamm S, Dippel B, Mihelcic D. The AIDA soot aerosol characterisation campaign 1999. J Aerosol Sci. 2003; 34:1277–1296. DOI: 10.1016/S0021-8502(03)00363-X

34. McDonald JD, Harrod KS, Seagrave JC, Seilkop SK, Mauderly JL. Effects of low sulfur fuel and a catalyzed particle trap on the composition and toxicity of diesel emissions. Environ Health Perspect. 2004; 112(13):1307–1312. DOI: 10.1289/ehp.7059 [PubMed: 15345344]

35. Bonvallot V, Baeza-Squiban a, Baulig a, Brulant S, Boland S, Muzeau F, Barouki R, Marano F. Organic compounds from diesel exhaust particles elicit a proinflammatory response in human airway epithelial cells and induce cytochrome p450 1A1 expression. Am J Respir Cell Mol Biol. 2001; 25(17):515–521. [PubMed: 11694458]

36. Totlandsdal AI, Refsnes M, Låg M. Mechanisms involved in ultrafine carbon black-induced release of IL-6 from primary rat epithelial lung cells. Toxicol Vitr. 2010; 24(1):10–20. DOI: 10.1016/j.tiv.2009.09.016

37. Vogel CFA, Sciullo E, Wong P, Kuzmicky P, Kado N, Matsumura F. Induction of proinflammatory cytokines and C-reative protein in human macrophage cell line U937 exposed to air pollution particulates. Environ Health Perspect. 2005; 113(11):1536–1541. DOI: 10.1289/ehp.8094 [PubMed: 16263508]

38. Nebert DW, Dalton TP, Okey AB, Gonzalez FJ. Role of aryl hydrocarbon receptor-mediated induction of the CYP1 enzymes in environmental toxicity and cancer. J Biol Chem. 2004; 279(23):23847–23850. DOI: 10.1074/jbc.R400004200 [PubMed: 15028720]

39. Øvrevik J, Refsnes M, Låg M, Holme J, Schwarze P. Activation of Proinflammatory Responses in Cells of the Airway Mucosa by Particulate Matter: Oxidant- and Non-Oxidant-Mediated Triggering Mechanisms. Biomolecules. 2015; 5(3):1399–1440. DOI: 10.3390/biom5031399 [PubMed: 26147224]

40. Deering-Rice CE, Romero EG, Shapiro D, Hughen RW, Light A, Yost GS, Veranth JM, Reilly CA. Electrophilic components of diesel exhaust particles (DEP) activate transient receptor potential ankyrin-1 (TRPA1): Probable mechanism of acute pulmonary toxicity for DEP. Chem Res Toxicol. 2012; 24(6):950–959. DOI: 10.1021/tx200123z.Electrophilic

41. Shapiro D, Deering-Rice CE, Romero EG, Hughen RW, Light AR, Veranth JM, Reilly CA. Activation of transient receptor potential ankyrin-1 (TRPA1) in lung cells by wood smoke particulate material. Chem Res Toxicol. 2013; 26(5):750–758. DOI: 10.1021/tx400024h [PubMed: 23541125]

42. Echavarria CA, Sarofim AF, Lighty JS, D'Anna A. Modeling and measurements of size distributions in premixed ethylene and benzene flames. Proc Combust Inst. 2009; 32(1):705–711.

43. Echavarria, Ca, Sarofim, AF., Lighty, JS., D'Anna, A. Evolution of soot size distribution in premixed ethylene/air and ethylene/benzene/air flames: Experimental and modeling study. Combust Flame. 2011; 158(1):98–104. DOI: 10.1016/j.combustflame.2010.07.021

44. Jaramillo IC, Gaddam CK, Vander Wal RL, Huang CH, Levinthal JD, Lighty JS. Soot oxidation kinetics under pressurized conditions. Combust Flame. 2014; 161(11):2951–2965. DOI: 10.1016/j.combustflame.2014.04.016

45. Ghiassi H, Toth P, Lighty JS. Sooting behaviors of n-butanol and n-dodecane blends. Combust Flame. 2014; 161(3):671–679. DOI: 10.1016/j.combustflame.2013.10.011

46. Camacho J, Lieb S, Wang H. Evolution of size distribution of nascent soot in n- and i-butanol flames. Proc Combust Inst. 2013; 34(1):1853–1860. DOI: 10.1016/j.proci.2012.05.100
47. Camacho J, Tao Y, Wang H. Kinetics of nascent soot oxidation by molecular oxygen in a flow reactor. Proc Combust Inst. 2015; 35(2):1887–1894. DOI: 10.1016/j.proci.2014.05.095
48. Abid AD, Camacho J, Sheen DA, Wang H. Quantitative measurement of soot particle size distribution in premixed flames - The burner-stabilized stagnation flame approach. Combust Flame. 2009; 156(10):1862–1870. DOI: 10.1016/j.combustflame.2009.05.010
49. Penn A, Murphy G, Barker S, Henk W, Penn L. Combustion-derived ultrafine particles transport organic toxicants to target respiratory cells. Environ Health Perspect. 2005; 113(8):956–963. DOI: 10.1289/ehp.7661 [PubMed: 16079063]
50. McEnally C, Köylü Ü, Pfefferle L, Rosner D. Soot volume fraction and temperature measurements in laminar nonpremixed flames using thermocouples. Combust Flame. 1997; 109(4):701–720.
51. Ku BK, Kulkarni P. HHS Public Access. 2015; :100–110. DOI: 10.1016/j.jaerosci.2012.01.002.Comparison
52. Agarwal AK, Gupta T, Kothari A. Particulate emissions from biodiesel vs diesel fuelled compression ignition engine. Renew Sustain Energy Rev. 2011; 15(6):3278–3300. DOI: 10.1016/j.rser.2011.04.002
53. Agarwal AK, Singh AP, Lukose J, Gupta T. Characterization of exhaust particulates from diesel fueled homogenous charge compression ignition combustion engine. J Aerosol Sci. 2013; doi: 10.1016/j.jaerosci.2012.12.005
54. Stabile L, Buonanno G, Ficco G, Scungio M. Smokers' lung cancer risk related to the cigarette-generated mainstream particles. J Aerosol Sci. 2017; 107:41–54. DOI: 10.1016/j.jaerosci.2017.02.005
55. Jaramillo IC, Gaddam CK, Vander Wal RL, Lighty JS. Effect of nanostructure, oxidative pressure and extent of oxidation on model carbon reactivity. Combust Flame. 2015; 162(5):1848–1856. DOI: 10.1016/j.combustflame.2014.12.006
56. Hermanns MI, Unger RE, Kehe K, Peters K, Kirkpatrick CJ. Lung epithelial cell lines in coculture with human pulmonary microvascular endothelial cells: development of an alveolo-capillary barrier in vitro. Lab Invest. 2004; 84(6):736–752. DOI: 10.1038/labinvest.3700081 [PubMed: 15077120]
57. Salomon JJ, Muchitsch VE, Gausterer JC, Schwagerus E, Huwer H, Daum N, Lehr CM, Ehrhardt C. The cell line NCl-H441 is a useful in vitro model for transport studies of human distal lung epithelial barrier. Mol Pharm. 2014; 11:995–1006. DOI: 10.1021/mp4006535 [PubMed: 24524365]
58. Daigneault M, Preston Ja, Marriott HM, Whyte MKB, Dockrell DH. The identification of markers of macrophage differentiation in PMA-stimulated THP-1 cells and monocyte-derived macrophages. PLoS One. 2010; 5(1)doi: 10.1371/journal.pone.0008668
59. O'Reilly MA, Gazdar AF, Clark JC, Pilot-Matias TJ, Wert SE, Hull WM, Whitsett JA. Glucocorticoids regulate surfactant protein synthesis in a pulmonary adenocarcinoma cell line. Am J Physiol - Lung Cell Mol Physiol. 1989; 257(6):L385–L392.
60. Cho A, Sioutas C, Miguel A, Kumagai Y, Schmitz D, Singh M, Eiguren-Fernandez A, Froines J. Redox activity of airborne particulate matter at different sites in the Los Angeles Basin. Env Res. 2005; 99(1):40–47. [PubMed: 16053926]
61. Harris SJ, Maricq MM. Signature size distributions for diesel and gasoline engine exhaust particulate matter. Journal of Aerosol Science. 2001; 32:749–764.
62. Maricq MM, Xu N. The effective density and fractal dimension of soot particles from premixed flames and motor vehicle exhaust. J Aerosol Sci. 2004; 35:1251–1274. DOI: 10.1016/j.jaerosci.2004.05.002
63. Matti Maricq M. Chemical characterization of particulate emissions from diesel engines: A review. J Aerosol Sci. 2007; 38(11):1079–1118. DOI: 10.1016/j.jaerosci.2007.08.001
64. Schwarze PE, Totlandsdal AI, Låg M, Refsnes M, Holme JA, Øvrevik J. Inflammation-Related Effects of Diesel Engine Exhaust Particles: Studies on Lung Cells In Vitro. Hindawi Publ. Corp. BioMed Res. Int. 2013; 2013:1–14.

65. Totlandsdal AI, Øvrevik J, Cochran RE, Herseth JI, Bølling AK, Låg M, Schwarze P, Lilleaas E, Holme Ja, Kubátová A. The occurrence of polycyclic aromatic hydrocarbons and their derivatives and the proinflammatory potential of fractionated extracts of diesel exhaust and wood smoke particles. J Environ Sci Health A Tox Hazard Subst Environ Eng. 2014; 49(4):383–396. DOI: 10.1080/10934529.2014.854586 [PubMed: 24345236]
66. Li N, Xia T, Nel AE. The role of oxidative stress in ambient particulate matter-induced lung diseases and its implications in the toxicity of engineered nanoparticles. Free Radic Biol Med. 2008; 44(9):1689–1699. DOI: 10.1016/j.freeradbiomed.2008.01.028 [PubMed: 18313407]
67. Donaldson K, Stone V, Borm PJA, Jimenez LA, Gilmour PS, Schins RPF, Knaapen AM, Rahman I, Faux SP, Brown DM, et al. Oxidative stress and calcium signaling in the adverse effects of environmental particles (PM10). Free Radic Biol Med. 2003; 34(11):1369–1382. DOI: 10.1016/S0891-5849(03)00150-3 [PubMed: 12757847]
68. González-Flecha B. Oxidant mechanisms in response to ambient air particles. Mol Aspects Med. 2004; 25:1–2. 169–182. DOI: 10.1016/j.mam.2004.02.017 [PubMed: 15051311]
69. Mazzoli-Rocha F, Fernandes S, Einicker-Lamas M, Zin WA. Roles of oxidative stress in signaling and inflammation induced by particulate matter. Cell Biol Toxicol. 2010; 26(5):481–498. DOI: 10.1007/s10565-010-9158-2 [PubMed: 20340042]
70. Totlandsdal AI, Cassee FR, Schwarze P, Refsnes M, Låg M. Diesel exhaust particles induce CYP1A1 and pro-inflammatory responses via differential pathways in human bronchial epithelial cells. Part Fibre Toxicol. 2010; 7(1):41.doi: 10.1186/1743-8977-7-41 [PubMed: 21162728]
71. Andrysík Z, Procházková J, Kabátková M, Umannová L, Simečková P, Kohoutek J, Kozubík A, Machala M, Vondráček J. Aryl hydrocarbon receptor-mediated disruption of contact inhibition is associated with connexin43 downregulation and inhibition of gap junctional intercellular communication. Arch Toxicol. 2013; 87(3):491–503. DOI: 10.1007/s00204-012-0963-7 [PubMed: 23085979]
72. Kumfer, B., Kennedy, I. The role of soot in the health effects of inhaled airborne particles. In: Bockhorn, H.D'Anna, A.Sarofim, AF., Wang, H., editors. Proceedings of an international workshop held in villa Orlandi; Anacapri. May 13–16; Karlsruhe University Press; 2007. p. 1-15.
73. Attia SM. Deleterious Effects of Reactive Metabolites. Oxid Med Cell Longev. 2010; 3(4):238–253. DOI: 10.4161/oxim.3.4.13246 [PubMed: 20972370]
74. Sadiktsis I, Koegler JH, Benham T, Bergvall C, Westerholm R. Particulate associated polycyclic aromatic hydrocarbon exhaust emissions from a portable power generator fueled with three different fuels - A comparison between petroleum diesel and two biodiesels. Fuel. 2014; 115:573–580.
75. Zhang ZH, Balasubramanian R. Physicochemical and toxicological characteristics of particulate matter emitted from a non-road diesel engine: Comparative evaluation of biodiesel-diesel and butanol-diesel blends. J Hazard Mater. 2014; 264:395–402. DOI: 10.1016/j.jhazmat.2013.11.033 [PubMed: 24316811]
76. Till M, Riebniger D, Schmitz HJ, Schrenk D. Potency of various polycyclic aromatic hydrocarbons as inducers of CYP1A1 in rat hepatocyte cultures. Chem Biol Interact. 1999; 117(2):135–150. DOI: 10.1016/S0009-2797(98)00105-7 [PubMed: 10190573]
77. Li N, Hao M, Phalen RF, Hinds WC, Nel AE. Particulate air pollutants and asthma: A paradigm for the role of oxidative stress in PM-induced adverse health effects. Clin Immunol. 2003; 109(3):250–265. DOI: 10.1016/j.clim.2003.08.006 [PubMed: 14697739]
78. Deng X, Zhang F, Rui W, Long F, Wang L, Feng Z, Chen D, Ding W. PM2.5-induced oxidative stress triggers autophagy in human lung epithelial A549 cells. Toxicol Vitr. 2013; 27(6):1762–1770. DOI: 10.1016/j.tiv.2013.05.004
79. Kocbach A, Totlandsdal AI, Låg M, Refsnes M, Schwarze PE. Differential binding of cytokines to environmentally relevant particles: A possible source for misinterpretation of in vitro results? Toxicol Lett. 2008; 176(2):131–137. DOI: 10.1016/j.toxlet.2007.10.014 [PubMed: 18079072]
80. Patel H, Eo S, Kwon S. Effects of diesel particulate matters on inflammatory responses in static and dynamic culture of human alveolar epithelial cells. Toxicol Lett. 2011; 200:1–2. 124–131. DOI: 10.1016/j.toxlet.2010.11.007 [PubMed: 20932884]

81. Tal TL, Simmons SO, Silbajoris R, Dailey L, Cho SH, Ramabhadran R, Linak W, Reed W, Bromberg PA, Samet JM. Differential transcriptional regulation of IL-8 expression by human airway epithelial cells exposed to diesel exhaust particles. Toxicol Appl Pharmacol. 2010; 243(1): 46–54. DOI: 10.1016/j.taap.2009.11.011 [PubMed: 19914270]

82. Reilly, CA. The role of TRP channels in the lung. In: McQueen, CA., editor. Comprehensive Toxicology. Elsevier; Oxford, UK: 2010. p. 129-149.

83. Lanosa MJ, Willis DN, Jordt S, Morris JB. Role of metabolic activation and the TRPA1 receptor in the sensory irritation response to styrene and naphthalene. Toxicol Sci. 2010; 115(2):589–595. DOI: 10.1093/toxsci/kfq057 [PubMed: 20176620]

84. Hussain S, Boland S, Baeza-Squiban A, Hamel R, Thomassen LCJ, Martens JA, Billon-Galland MA, Fleury-Feith J, Moisan F, Pairon JC, et al. Oxidative stress and proinflammatory effects of carbon black and titanium dioxide nanoparticles: Role of particle surface area and internalized amount. Toxicology. 2009; 260:1–3. 142–149. DOI: 10.1016/j.tox.2009.04.001 [PubMed: 19464563]

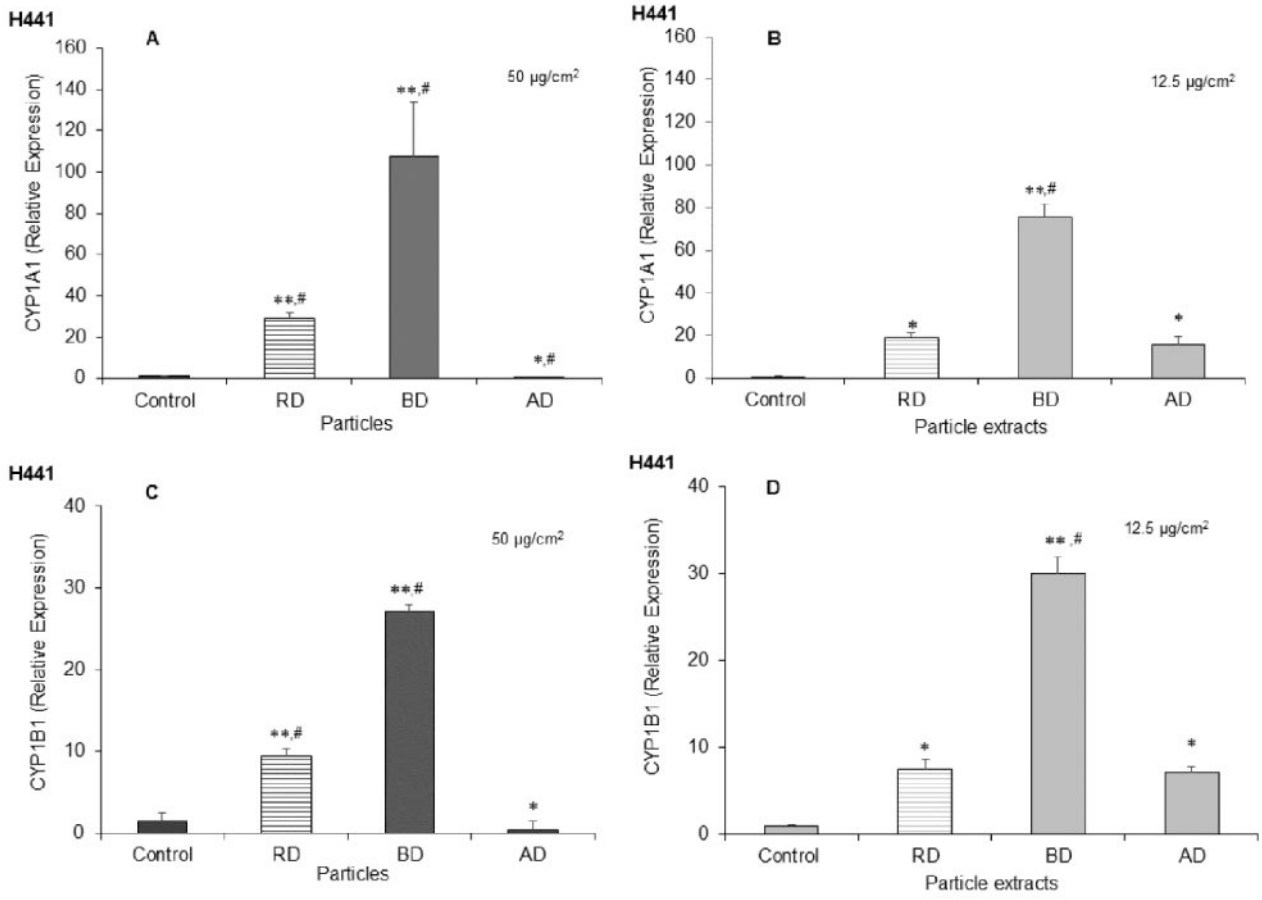

Figure 1.

CYP1A1 and CYP1B1 mRNA expression due to treatment with particles and particle extracts. Human H441 cells were exposed to cdPM (A and C) and cdPM extracts (B and D) or medium alone for 24h. Treatments were = 50 μg/cm^2 (200 μg/mL) for particles and 12.5 μg/cm^2 (50 μg/mL) for particle extracts. Control = medium + DMSO (0.1% v/v). Data are expressed as mean ± SEM (n=3) and are representative of 3 independent experiments. *Indicates statistical significance (*$p<0.05$; **$p<0.005$) relative to the control (one-way ANOVA). #Indicates difference ($p<0.05$) relative to other marked groups (one-way ANOVA with Tukey's HSD). Solid columns indicate cdPM from the FFB, and hatched columns indicate reference diesel.

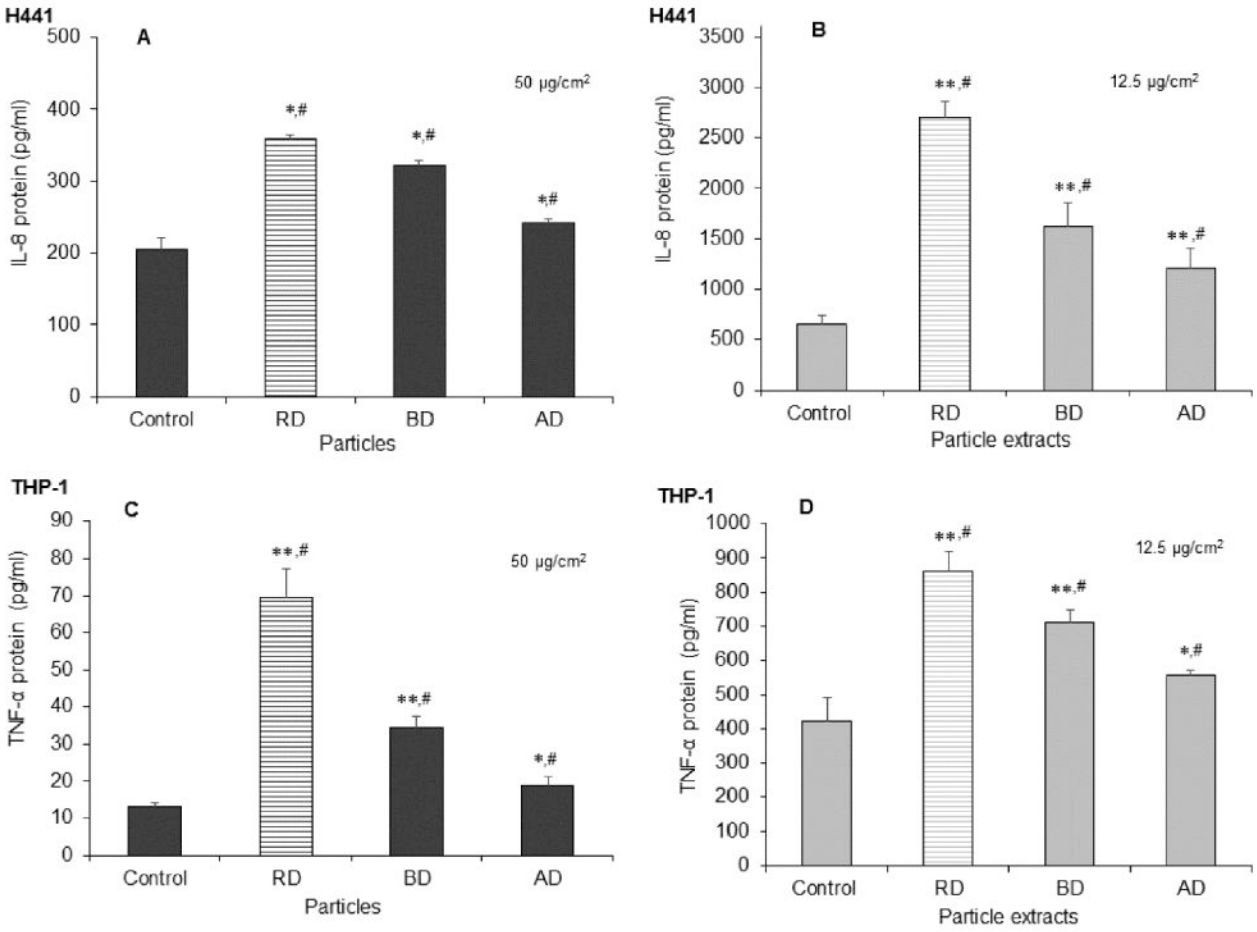

Figure 2.

IL-8 and TNFα cytokine secretion by H441 and THP-1 cells, respectively, in response to cdPM and cdPM extracts. Human H441 (A and B) and THP-1 (C and D) cells were exposed to cdPM (A and C) and cdPM extracts (B and D) or medium alone for 24h. Treatments = 50 µg/cm^2 (200 µg/mL) for particles and 12.5 µg/cm^2 (50 µg/mL) for particle extracts. Control = medium + DMSO (0.1% v/v). Data are expressed as mean ± SEM (n=3) and are representative of 3 experiments. *Indicates statistical significance (*$p<0.05$; **$p<0.005$) relative to the control (one-way ANOVA). #Indicates difference ($p<0.05$) relative to other marked groups (one-way ANOVA with Tukey's HSD). Solid columns indicate cdPM from the FFB, and hatched columns indicate reference diesel.

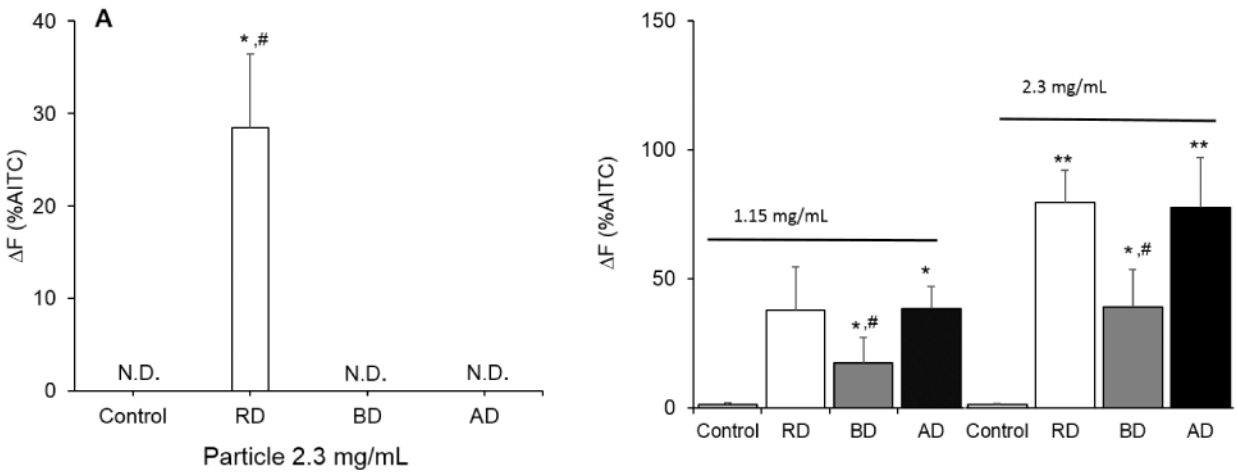

Figure 3.

Activation of human TRPA1-mediated calcium influx in TRPA1-overexpressing HEK-293 reporter cells by cdPM (A) and cdPM extracts (B). Cells were treated for 1 min with constant monitoring of intracellular fluorescence intensity with 25 μL of a 3× suspension of cdPM or corresponding cdPM extracts. Control = medium + DMSO (2% v/v), cdPM suspensions = 2.3 mg/mL equivalent to 180 μg/cm^2 and 1.15 mg/mL equivalent to 90 μg/cm^2. Data are expressed as mean ± SEM (n=3) and are representative of 3 experiments. N.D. indicates non-detect. *Indicates statistical significance (*$p<0.05$; **$p<0.005$) relative to the control. #Indicates difference ($p<0.05$) relative to other marked groups. The results in Panel A were analyzed by one-way ANOVA, and the results in Panel B were analyzed by two-way ANOVA with with Dunnett's a post-hoc analysis. Solid columns indicate cdPM from the FFB, and hatched columns indicate reference diesel.

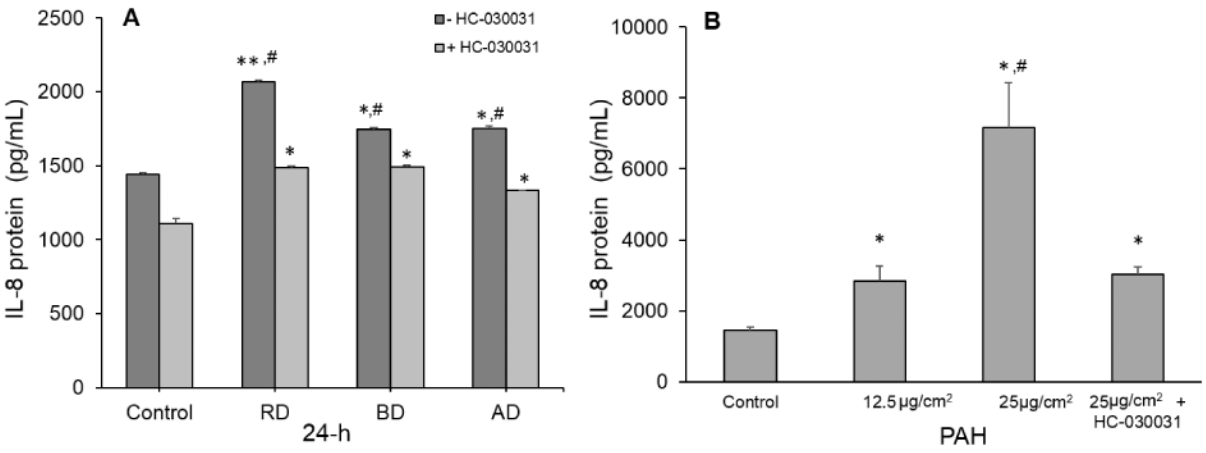

Figure 4.

The role of TRPA1 in IL-8 cytokine secretion by cdPM (A; 12.5 µg/cm^2 or 50 µg/mL) and PAHs (B; 12.5 and 25 µg/cm^2 or 50 and 100 µg/mL). Cells were treated and assayed as in Fig. 2 in the presence and absence of the TRPA1 antagonist HC-030031 (25 µM). *Indicates statistical significance (*$p<0.05$; **$p<0.005$) relative to the control. #Indicates difference ($p<0.05$) relative to either RD or AD groups. Solid columns indicate cdPM from the FFB, and hatched columns indicate reference diesel.

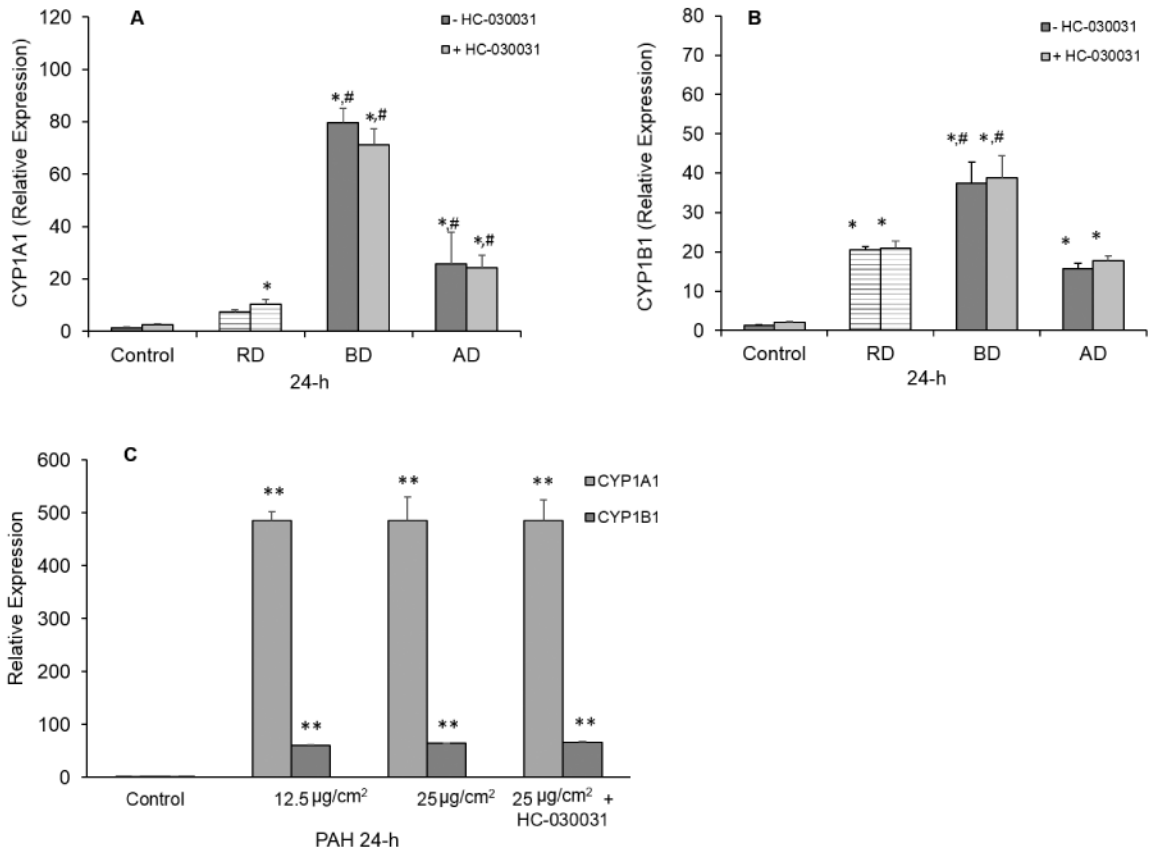

Figure 5.

Effects of the TRPA1 antagonist HC-030031 on CYP1A1 and 1B1 mRNA expression by the cdPM extracts and PAH mixture. Human H441 cells were exposed to cdPM extracts (12.5 and 25 μg/cm^2 or 50 and 100 μg/mL) for 24h. Control = medium + DMSO (0.1% v/v). HC-030031 (25μM) was added to the cells at the same time as the extracts. Cells were analyzed for CYP1A1 mRNA transcript levels (A), CYP1B1 mRNA transcript levels (B) and CYP1A1 and 1B1 mRNA transcript levels after PAH treatment (**C**). Data are expressed as mean ± SEM (n=3). *Indicates statistical significance (*p<0.05; **p<0.005) relative to the control. #Indicates difference (p<0.05) relative to other marked groups. Solid columns indicate cdPM from the FFB, and hatched columns indicate reference diesel.

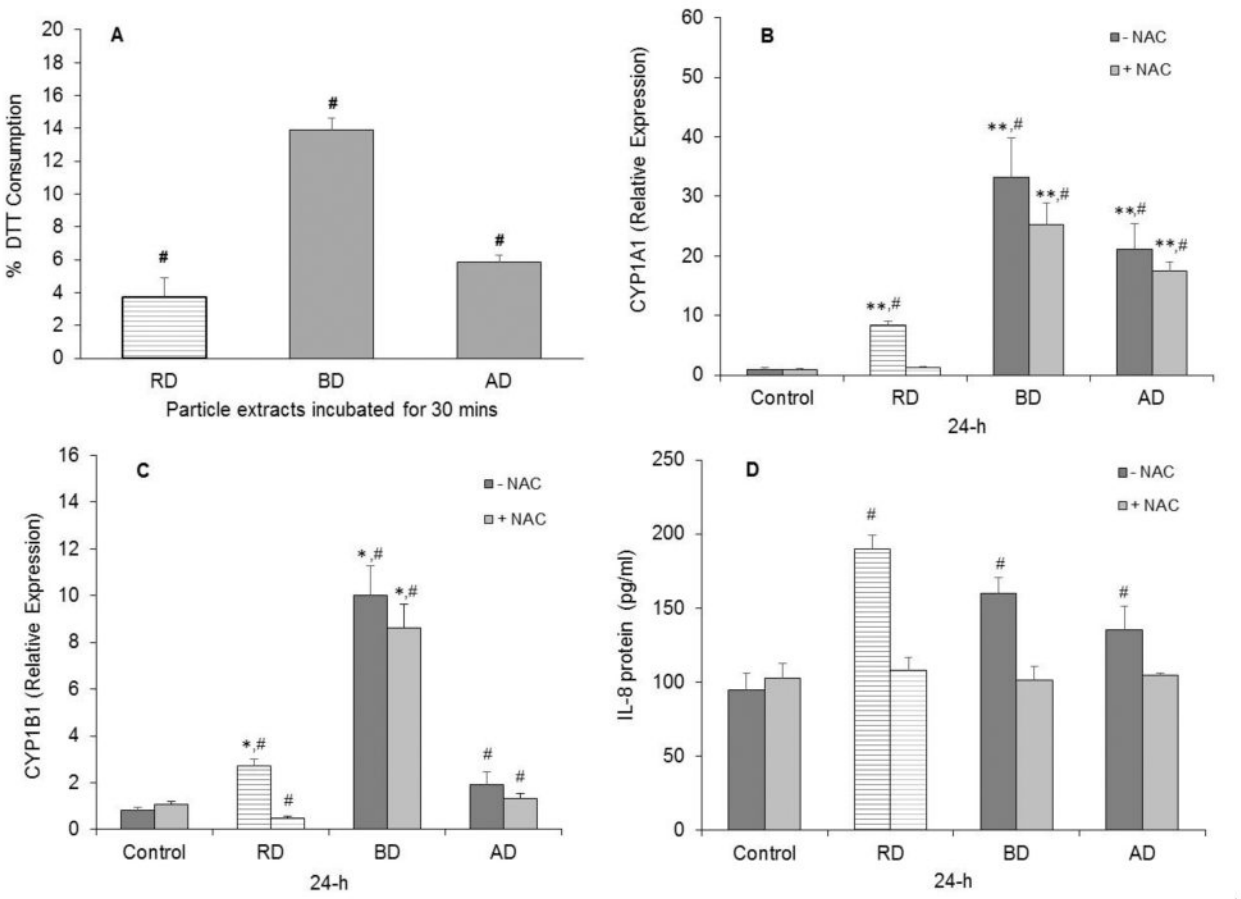

Figure 6.

Oxidative potential and effects of the antioxidant NAC on cellular responses to cdPM. Oxidative potential/electrophile content of cdPM extracts as measured by DTT oxidation. Data are expressed as %DTT consumed over a 30-minute period (A). Data are represented as mean ± SEM (n=6). *Indicates statistical significance (*p<0.05; **p<0.005) relative to the control groups. (B-D) Effect of NAC on CYP1A1 mRNA expression (B), CYP1B1 mRNA expression (C), and IL-8 cytokine secretion by H441 cells (D). Cells were exposed to particle extracts (12.5 μg/cm^2 or 50 μg/mL) for 24h. Control = medium + DMSO (0.1% v/v). Data are expressed as mean ± SEM (n=3) and are representative of 2 independent experiments. #Indicates difference (p<0.05) relative to other marked groups. Solid columns indicate cdPM from the FFB, and hatched columns indicate reference diesel. Lighter colored bars indicate NAC addition while darker bars correspond to results without NAC addition.

Table 1

Particle size, surface area, and ethanol-extractable material content

Sample Identity	Particle size distribution (nm)	Median particle size** (nm)	Surface Area (m^2/g)	Ethanol Soluble Mass## (%)
BD	2-50	26±3	384*	20 ± 2
AD	2-80	41±5	125*	12 ± 3
RD	N.D.	28±3	80#	8 ± 3

*Measured by SEM;

#Obtained from NIST Certificate of Analysis. N.D. = Not determined.

**Statistically significant differences: BD > AD and BD > RD by one-way ANOVA with Tukey post hoc analysis and 95% confidence.

##Statistically significant differences: BD > AD and BD > RD by one-way ANOVA with Turkey and 95% confidence.

Table 2
16-PAH mass concentration (μg/g) for the extracts

Compound Name	RD (μg/g)	BD (μg/g)	AD (μg/g)
2-ring PAHs			
Naphthalene	5.45	2.17	0.24
total	***5.45***	***2.17***	***0.24***
3-ring PAHs			
Acenaphthylene	0.68	0.50	0.23
Acenaphthene	1.00	0.37	0.35
Fluorene	0.91	1.62	0.13
Phenanthrene	14.55	8.33	14.52
Anthracene	0.73	0.65	1.29
total	***17.86***	***11.47***	***16.52***
4-ring PAHs			
Fluoranthene	17.73	4.33	22.58
Pyrene	0.95	7.00	14.52
total	***18.68***	***11.33***	***37.10***
5-ring PAHs			
Benzo(a)anthracene	0.68	2.17	0.24
Chrysene	6.82	1.83	1.94
Benzo[b]fluoranthene	8.18	8.33	7.26
Benzo[k]fluoranthene	1.18	2.83	3.39
Benzo[a]pyrene	1.09	12.67	12.90
Indeno[1,2,3-cd]pyrene	0.86	10	6.45
Dibenzo[a,h]anthracene	1.27	0.47	0.45
Benzo[g,h,i]perylene	0.86	3.17	6.13
total	**20.95**	**41.47**	**38.76**
Total PAH Content	**62.95**	**66.43**	**92.61**

The extracted fraction in BD was 20 ±2 %, AD 12 ±3% and RD 8±3%.